Microchimica Acta (2020) 187: 115
https://doi.org/10.1007/s00604-019-4070-9

ORIGINAL PAPER

# Colorimetric determination of the activity of alkaline phosphatase by exploiting the oxidase-like activity of palladium cube@$CeO_2$ core-shell nanoparticles

Jiawei Wang[1] · Pengjuan Ni[1] · Chuanxia Chen[1] · Yuanyuan Jiang[1] · Chenghui Zhang[1] · Bo Wang[1] · Bingqiang Cao[2] · Yizhong Lu[1]

Received: 29 July 2019 / Accepted: 6 December 2019 / Published online: 9 January 2020


## Abstract

Core-shell palladium cube@$CeO_2$ (Pd cube@$CeO_2$) nanoparticles are shown to display oxidase-like activity. This is exploited in a method for determination of the activity of alkaline phosphatase (ALP). The Pd cube@$CeO_2$ nanoparticles were thermally synthesized from $Ce(NO_3)_3$, L-arginine and preformed Pd cube seeds in water. The Pd cube@$CeO_2$ nanoparticles catalyze the oxidation of 3,3′,5,5′-tetramethylbenzidine (TMB) by oxygen. This results in the formation of oxidized TMB (oxTMB) with an absorption peak at 652 nm. Ascorbic acid (AA) is generated from the hydrolysis of L-ascorbic acid 2-phosphate (AAP) catalyzed by ALP. It can reduce oxTMB to TMB, and this results in a decrease of the absorbance. The method allows for quantitative determination of the activity of ALP in the range from 0.1 to 4.0 $U{\cdot}L^{-1}$ and with a detection limit down to 0.07 $U{\cdot}L^{-1}$. Endowed with high sensitivity and selectivity, the assay can quantify ALP activity in biological system with satisfactory results.

**Keywords** Alkaline phosphatase · Ascorbic acid · Cerium oxide · Pd cube · 3,3′,5,5′-tetramethylbenzidine · Oxidase mimic · Colorimetric assay · Ascorbic acid 2-phosphate · Nanozyme

## Introduction

Alkaline phosphatase (ALP) plays a key role in catalytic dephosphorilation [1]. ALP promotes the hydrolysis of monoester phosphates, which is capable of producing phosphates and products containing free hydroxy groups [2]. ALP plays an important role in signal transduction and regulation of intracellular processes [3, 4]. Many methods have been reported for ALP detection, including electrochemistry [5], colorimtry [6], electrochemiluminescence [7], fluorimetry [8] and surface enhanced Raman scattering [9].

Colorimetry has become the preferred method for clinical applications due to its simplicity, readability, low cost, fast response and high throughput [10]. The most widely used colorimetric assay for ALP activity detection is based on the conversion of colorless *p*-nitrophenylphosphate (pNPP) to yellow *p*-nitrophenol. The method is simple and effective, which has been considered as a standard method for ALP activity monitoring. However, pNPP is very sensitive to light and is prone to spontaneous hydrolysis, both of which lead to inaccurate measurement results [11]. Consequently, developing sensitive, selective and accurate method for ALP detection is of great importance. In the past few years, nanozymes, a class of mimic enzymes that show both the unique properties of nanomaterials and catalytic functions, have been reported to replace natural enzymes. So far, many materials have been defined as nanozymes, such as Au@Pd nanoparticles [12], Au@Pt nanostructures [13], Prussian blue nanocubes [14], $Fe_3O_4$ nanoparticles [15–17] and Pt nanoparticles [18, 19]. Compared with natural enzymes,

**Electronic supplementary material** The online version of this article (https://doi.org/10.1007/s00604-019-4070-9) contains supplementary material, which is available to authorized users.

✉ Pengjuan Ni
mse_nipj@ujn.edu.cn

✉ Yuanyuan Jiang
mse_jiangyy@ujn.edu.cn

✉ Yizhong Lu
mse_luyz@ujn.edu.cn

[1] School of Materials Science and Engineering, University of Jinan, Jinan 250022, China

[2] Department of Physics and Institute of Laser, Qufu Normal University, Qufu 273165, China

nanozymes are more stable and cheaper, which shows great potential in biosensing [20, 21]. Recent studies have shown that ALP assays can be easily achieved by modulating the catalytic capabilities of nanozymes. For example, Wu et al. have reported a colorimetric assay for ALP activity detection based on the peroxidase-like activity of Prussian blue nanoparticles [22]. Jiang et al. reported a colorimetric assay for the detection of ALP activity by employing copper (II)-based metal-organic frameworks as peroxidase mimic and pyrophosphate as recognition element [23]. Though these methods using peroxidase mimetics show high sensitivity, they are limited by the utilization of unstable $H_2O_2$. Therefore, many efforts have been made to develop colorimetric assays for ALP detection using oxidase mimetics since they can directly oxidize 3,3′,5,5′-tetramethylbenzidine (TMB) without the addition of $H_2O_2$, making it much simpler [10]. However, there are few types of oxide mimetics that have been reported so far.

We describe a colorimetric assay for ALP activity based on the oxidase-like activity of Pd cube@$CeO_2$ nanoparticles. $CeO_2$ nanoparticlesshow low oxidase-like activity [24, 25]. Therefore, we utilize the core-shell composite of Pd cube and $CeO_2$ to ensure that the material has strong oxidase-like activity and shows high sensitivity for ALP detection. Pd cube@$CeO_2$ nanoparticles show oxidase-like activity that can directly oxidize TMB to oxidized TMB (oxTMB), resulting in a bluish solution and an intense absorption peak at 652 nm. ALP can catalyze the hydrolysis of L-ascorbic acid 2-phosphate (AAP) to produce ascorbic acid (AA) which can reduce oxTMB to TMB [26]. Consequently, the solution color turns to light blue with a decreased absorption intensity at 652 nm. On the basis of the above facts, a colorimetric assay for ALP detection is developed.

## Experimental section

### Chemicals and materials

Polyvinylpyrrolidone (PVP, MW ≈ 55,000), KBr, 3,3′,5,5′-tetramethylbenzidine (TMB), ALP (EC 3.1.3.1), AAP and AA were purchased from Sigma-Aldrich (St. Louis, USA, www.sigmaaldrich.com). $Na_2PdCl_4$ was obtained from Aladdin Reagent company (Shanghai, China,www.aladdin-e.com). L-arginine was purchased from Shanghai Macklin Biochemical Co., Ltd. (Shanghai, China, www.macklin.cn). $Ce(NO_3)_3{\cdot}6H_2O$ was supplied by Alfa Aesar (Tianjin, China, www.alfa.com). The water used in all experiments was supplied by a water purifier nanopure water system (18.2 MΩ cm). All chemicals were used as received without further purification.

### Materials characterization

The UV-vis absorption spectra were recorded on a UV-8000 spectrophotometer (ShanghaiMetash Instruments Co.,Ltd., China, www.metash.com). Transmission electron microscope (TEM) measurements were performed using a JEM 1400 (JEOL, Ltd., Japan, www.jeol.co.jp) at an acceleration voltage of 80 kV. High resolution transmission electron microscopic (HRTEM) measurements were performed using a JEM-2100 (JEOL Ltd., Japan, www.jeol.co.jp) at an acceleration voltage of 200 kV. The X-ray diffraction patterns of the products were collected on a Rigaku Ultima IV (Japan, www.rigaku.com) with an operation voltage and current maintained at 40 kV and 40 mA. The X-ray photoelectron spectroscopy (XPS) were performed by using a VG Thermo ESCALAB 250 spectrometer (VG Scientific, www.pdf.directindustry.com) operated at 120 W. The binding energy was calibrated against the carbon 1 s line.

### Detection assay procedure

10 μL of ALP with different activities, 10 μL of AAP (10 mM), 70 μL of Tris-HCl buffer (pH = 9.0, 10 mM) and 10 μL of $MgCl_2$ solution (50 mM) were sequentially introduced to 1.5 mL centrifuge tube. After thoroughly mixing and incubating at 37 °C for 30 min, 100 μL of Pd cube@$CeO_2$ nanoparticles (0.25 mg·mL$^{-1}$), 100 μL of TMB (5 mM) and 700 μL of acetic acid buffer (pH = 4.0, 10 mM) were added and incubated at 37 °C for another 10 min. Finally, the solution was transferred for the UV-vis absorption spectral measurements.

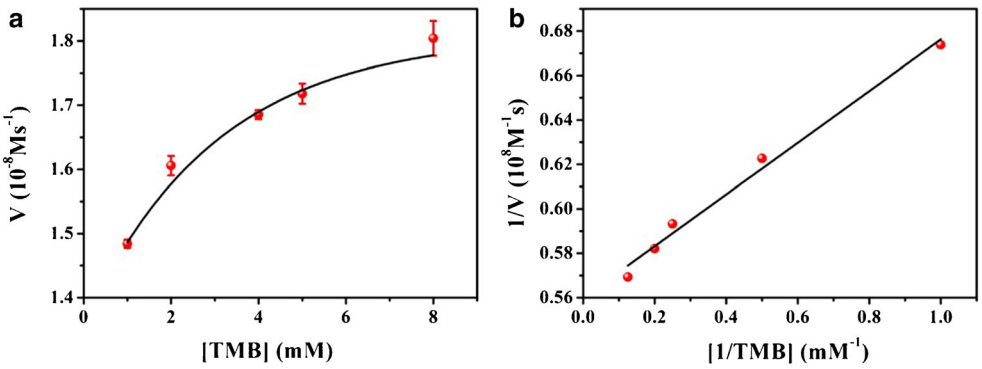


**Fig. 1** Kinetic assays of TMB oxidation by Pd cube@$CeO_2$ nanoparticles. **a** The fit based on Michaelis-Menten kineticsequation. **b** The corresponding Lineweaver-Burk plot

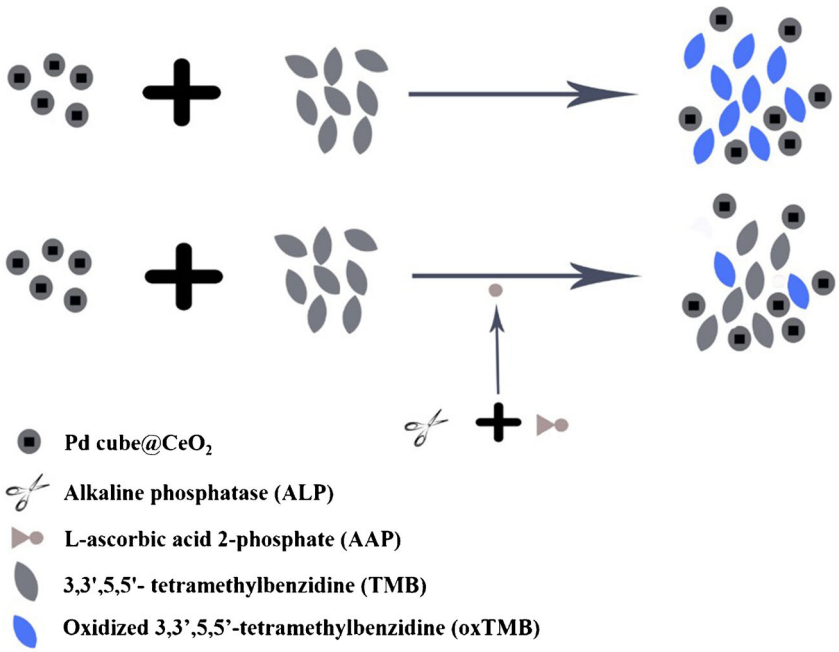


**Scheme 1** Schematic illustration of the detection principle of this method based on the oxidase-like activity of Pd cube@$CeO_2$ core-shell nanoparticles

## Results and discussion

Highly monodisperse Pd cube@$CeO_2$ composites are prepared by L-arginine-triggered self-assembly of $CeO_2$ on Pd cube. The material characterization part is shown in Fig. S1-S3. Typically, monodisperse Pd cubes with size of 12 nm are synthesized based on previous work (Fig. S1). And then, the Pd cube@$CeO_2$ nanoparticles are synthesized by heating the mixture of $Ce(NO_3)_3$, L-arginine, and pre-synthesized Pd cube at 80 °C for 3 h [27].

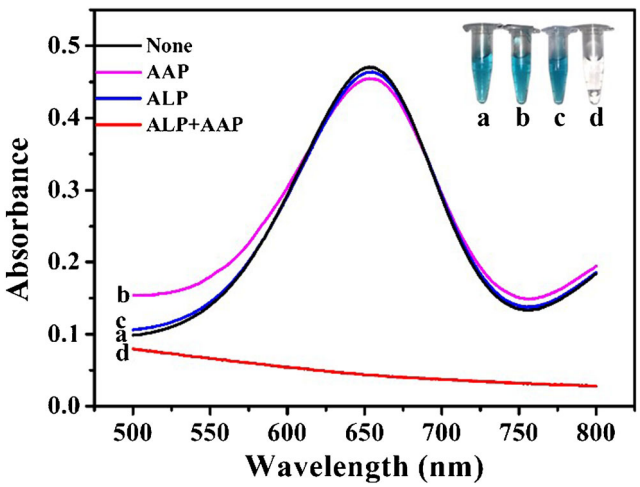


**Fig. 2** UV-vis absorption spectra of the detection systemin the absence (**a**) and presence of AAP (**b**), ALP (**c**), ALP and AAP (**d**). Inset shows the corresponding photos

### Kinetics of 3,3′,5,5′-tetramethylbenzidine (TMB) oxidation

In order to quantitatively evaluate the intrinsic oxidase-like activity of Pd cube@$CeO_2$ core-shell nanoparticles, we study the steady-state kinetic by varying the concentrations of TMB. The kinetic parameter for Pd cube@$CeO_2$ nanoparticles is determined by fitting the data of Fig. 1a into Michaelis-Menten equation. The initial velocity can be calculated by using the molar absorption coefficient of 3900 $M^{-1}$ $cm^{-1}$ for oxTMB. Michaelis-Menten constant ($K_m$) is the substrate concentration at which the reaction rate is half-maximum. A smaller $K_m$ indicates a stronger binding affinity of enzyme to substrate and hence often leads to a higher enzymatic activity [28]. The $K_m$ value can be obtained from the Lineweaver-Burk plot. From Fig. 1b, $K_m$ value is calculated to be 0.21 mM, which is lower than the $K_m$ values mentioned in previous report [25]. It indicates that Pd cube@$CeO_2$ nanoparticles show good affinity to TMB.

### Detection mechanism

The Pd cube alone is not sensitive to the detection of ALP (Fig. S4), so the Pd cube@$CeO_2$ core-shell nanoparticles are adopted. The detection principle of Pd cube@$CeO_2$ nanoparticles for ALP is shown in Scheme 1. Pd cube@$CeO_2$ nanoparticles show strong oxidase-like activity, which can oxidize TMB to oxTMB without the need for $H_2O_2$ and result in a strong absorption peak centered

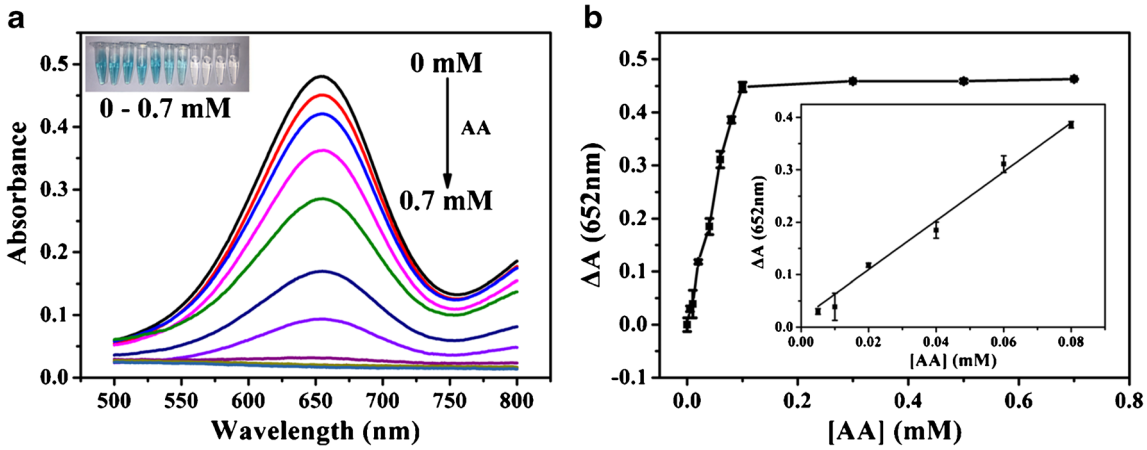


**Fig. 3** **a** UV-vis absorption spectra of Pd cube@$CeO_2$nanoparticles-TMB in the presence of various concentrations of AA (from top to down: 0, 0.005, 0.01, 0.02, 0.04, 0.06, 0.08, 0.1, 0.3, 0.5and 0.7 mM). Inset shows the photos of the corresponding solutions. **b** AA concentration dependent changes of the absorption intensity at 652 nm. Inset shows the liner relationship between the ΔA and AA concentration

at 652 nm (a, Fig. 2). When either AAP or ALP is introduced into detection assay, the changes of solution color and absorbance is negligible compared to blank solution (b and c, Fig. 2). After both AAP and ALP are added to the detection system, the solution turns to colorless and the absorption intensity at 652 nm decreases obviously (d, Fig. 2), which is attributed to the fact that AA generating form ALP-catalyzed hydrolysis of AAP can inhibit the oxidation of TMB [22, 29]. Based on the changes of solution colors and absorbance, this method can be used for ALP detection. The method does not involve $H_2O_2$ in the reaction, making it much simpler.

## Optimization of assay conditions

Before the application of this assay for ALP activity detection, several parameters such as pH value of buffer, incubation time, the concentrations of Pd cube@$CeO_2$ nanoparticles, TMB and AAP should be optimized. We utilize ΔA (ΔA = $A_0$-A) as the criterion to optimize the detection conditions, where $A_0$ and A are the absorbance at 652 nm of the detection system in the absence and presence of ALP, respectively.

### Optimization of pH

In order to determine the effect of pH values on ALP detection, we performed the assay in acetic acid buffer with different pH values (3.6–5.6). As shown in Fig. S5, with the increase of pH values, $A_0$ increases firstly and then decreases, while A keeps almost constant in the whole pH range. When the pH is 4.0, ΔA reaches a maximum value.

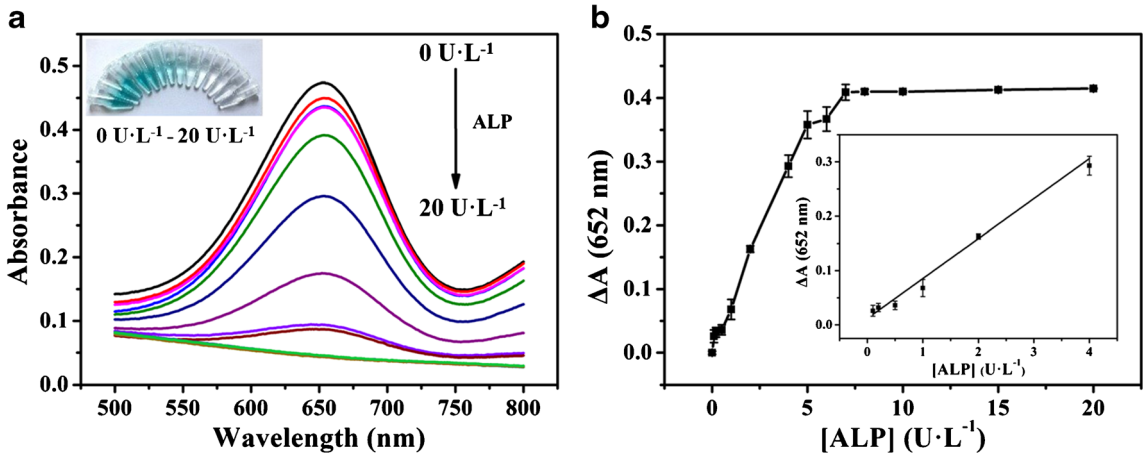


**Fig. 4** **a** UV-vis absorbance spectra of Pd cube@$CeO_2$nanoparticles-TMB in the absence and presence of various concentrations of ALP (from up to down: 0, 0.1, 0.2, 0.5, 1, 2, 4, 5, 6, 7, 8, 10,15, and 20 $U{\cdot}L^{-1}$), the inset show the photos of corresponding solutions. **b** ALP concentration dependent changes of the absorption intensity at 652 nm. Inset shows the liner relationship between the ΔA and ALP concentration

**Table 1** Comparison of the analytical performance of different methods for ALP detection

| Biosensing materials | Analytical method | Detection limit ($U \cdot L^{-1}$) | Linear range ($U \cdot L^{-1}$) | Reference |
|---|---|---|---|---|
| $Ce_3(PO_4)_4$ | Flourimetry | 2.3 | 0–50 | [10] |
| AuNCs | Flourimetry | 0.002 | 0.1–100 | [30] |
| NGQDs[a] | Flourimetry | 0.07 | 0.1–5 | [1] |
| coumarin@Tb-GMP | Flourimetry | 10 | 25–200 | [31] |
| $Ce^{3+}$-ATP-Tris | Flourimetry | 0.1 | 0.1–10 | [32] |
| Au@Ag NPs-GQDs | Flourimetry | 0.005 | 0.01–2 | [33] |
| Au@Ag NPs-GQDs | Colorimetry | 0.009 | 0.01–6 | [33] |
| AuNRs | Colorimetry | 0.01 | 0.01–0.4 | [6] |
| PB NCs | Colorimetry | 0.23 | 0.6–6 | [22] |
| CoOOH nanoflakes | Colorimetry | 0.026 | 0.04–160 | [34] |
| Pd cube@$CeO_2$ | Colorimetry | 0.07 | 0.1–4 | This work |

[a] nitrogen-dopedgraphene quantum dots

### Optimization of incubation time

Different reaction time has a great influence on the experimental results, and the effects of time (5, 10, 15, 20, 25 min) are investigated (Fig. S6A). When the reaction time is 10 min, the largest ΔA is obtained (Fig. S6B).

### Optimization of Pd cube@$CeO_2$ concentration

Different concentrations of Pd cube@$CeO_2$ nanoparticles represent different oxidizing ability of the detection system. We select samples with concentrations of 0.01, 0.025, 0.05, and 0.075 $mg \cdot mL^{-1}$ (Fig. S7A). When the concentration of Pd cube@$CeO_2$ nanoparticles is 0.025 $mg \cdot mL^{-1}$, ΔA gets the maximum value (Fig. S7B).

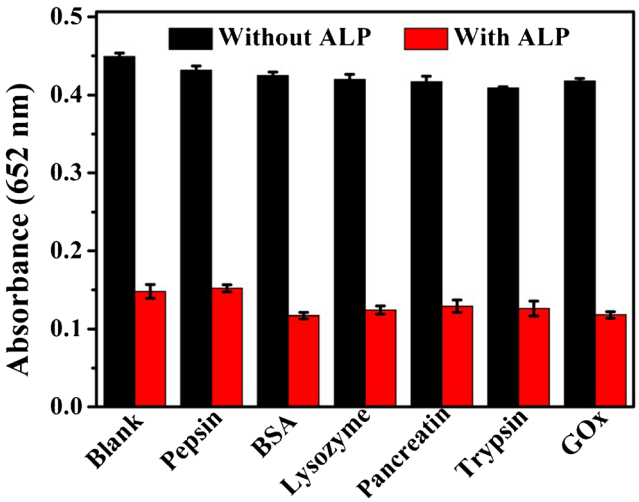


**Fig. 5** The absorbance of this detection assay in the presence of possible interfering substances only or coexistence with ALP. The final concentrations of these substances are 5 $U \cdot L^{-1}$, BSA are 100 $\mu g \cdot mL^{-1}$.Error bars indicate the standard deviation of three independent measurements

### Optimization of TMB concentration

To determine the effect of TMB concentration on the sensitivity of the detection system, we chosen different concentrations of TMB from 0.1 to 0.9 mM. As shown in Fig. S8, too high or too low concentration of TMB is not conducive to improving ΔA. Both $A_0$ and A increase with increasing TMB concentration (Fig. S8A). When the TMB concentration is 0.5 mM, ΔA reaches a maximum value (Fig. S8B).

### Optimization of AAP concentration

To test the effect of AAP concentration on the sensitivity of the detection system, we select different concentrations of AAP from 0 to 0.25 mM (Fig. S9A). When the AAP concentration is 0.1 mM, the ΔA value is the largest (Fig. S9B).

## Application of this method to the determination of AA and ALP activity

Under the optimum conditions, the Pd cube@$CeO_2$ core-shell nanoparticles-TMB system is used to detect AA based on its oxidase-like activity. An obvious color change from dark blue to light blue is found with the increasing concentrations of AA (inset of Fig. 3a). In addition, as the concentration of AA increases, the UV-vis absorption intensity at 652 nm decreases gradually (Fig. 3a). As shown in Fig. 3b, a good linear relationship between ΔA and AA concentration can be obtained in the range from 0.005 to 0.08 mM. The linear regression equation is $\Delta A = 4.668\,[AA] + 0.016$ ($R^2 = 0.994$) with a detection limit down to 1.3 μM.

In order to evaluate the performance of this method for ALP detection, the color changes of the detection assay before and after the introduction of various concentrations of ALP are recorded by a digital camera. Obvious color change from dark blue to light blue is found with the increasing

**Table 2** Determination of ALP in 100-fold diluted human serum samples

| Samples | Added ($U{\cdot}L^{-1}$) | Found ($U{\cdot}L^{-1}$) | pNPP assay ($U{\cdot}L^{-1}$) | Recovery (%) | RSD ($n = 4$, %) |
|---|---|---|---|---|---|
| 1 | 2 | 2.07 ± 0.14 | 1.96 ± 0.18 | 103.5 | 6.8 |
| 2 | 4 | 3.88 ± 0.12 | 4.02 ± 0.13 | 97.0 | 3.1 |

concentrations of ALP (inset of Fig. 4). The UV-vis absorption spectra of the system after the addition of different concentrations of ALP are also recorded. As the concentration of ALP increases, the absorbance at 652 nm decreases gradually (Fig. 4a). As shown in Fig. 4b, a good linear relationship between ΔA and the ALP concentration in the range from 0.1 to 4 $U{\cdot}L^{-1}$ is obtained. The linear regression equation is $\Delta A = 0.074\,[ALP] + 0.012$ ($R^2 = 0.984$) with a detection limit down to 0.07 $U{\cdot}L^{-1}$. Then, we compare the linear range and detection limit of this method with previously reported methods. The corresponding results are shown in Table 1. The analytical performances of our method are comparable or even better than reported methods.

### Selectivity

To demonstrate the selectivity of this assay for ALP, we firstly investigate the effects of possible interferences (pepsin, BSA, lysozyme, panceratin, trypsin and GOx). As shown in Fig. 5, when other enzymes and proteins are individually added to the sensing system, no significant change in the absorbance is observed.While the absorbance at 652 nm decreases significantly after ALP is added individually or simultaneously with other interfering substances. Then, we study other interfering substances that may be present in human serum, including AA, L-cysteine (Cys), uric acid (UA), glutathione (GSH) and L-homocysteine (HCy). As shown in Fig. S10, the absorbance of the detection system keep almost unchanged after the addition of interfering substances. These results indicate that the detection assay has high selectivity for ALP detection.

### Real sample analysis

In order to evaluate the practical application of our proposed method, the colorimetric assay is used to analyze ALP in human serum samples. Serum samples are diluted 100-fold and detected by using standard addition method. The solution is awakened to determine the UV-vis absorption peak after adding different concentrations of ALP (2 $U{\cdot}L^{-1}$ and 4 $U{\cdot}L^{-1}$). As shown in Table 2, the recoveriesare in the range from 97.0% to 103.5% with the RSD ranging from 3.1% to 6.8%. The experimental results are quite satisfactory, indicating that the method has great potential in real sample detection.

## Conclusion

We have established a colorimetric method for ALP activity detection based on the high oxidase-like activity of Pd cube@$CeO_2$ nanoparticles. This method shows high sensitivity, good selectivity and great potential to detect ALP in real samples, which provides good practicability and reliability for clinical detection of ALP activity. This assay may not only provide a new idea for construction of nanozymes with high oxidase-like activity, but also broaden the applications of oxidase mimetics.The limitation of the detection system is that it cannot distinguish the iso-enzymes of ALP in human plasma.

**Acknowledgments** This work was financially supported by the National Natural Science Foundation of China (21705056, 21904048, 21902061 and 21902062), the Young Taishan Scholars Program (tsqn201812080), the Natural Science Foundation of Shandong Province (ZR2019YQ10, ZR2017MB022, ZR2018BB057 and ZR2018PB009) and the Doctoral Funds of University of Jinan (160100445).

## References

1. Liu J, Tang D, Chen Z, Yan X, Zhong Z, Kang L, Yao J (2017) Chemical redox modulated fluorescence of nitrogen-doped graphene quantum dots for probing the activity of alkaline phosphatase. Biosens Bioelectron 94:271–277
2. Sun J, Hu T, Chen C, Zhao D, Yang F, Yang X (2016) Fluorescence immunoassay system via enzyme-enabled in situ synthesis of fluorescent silicon nanoparticles. Anal Chem 88:9789–9795
3. Park K, Lee C, Park H (2014) A sensitive dual colorimetric and fluorescence system for assaying the activity of alkaline phosphatase that relies on pyrophosphate inhibition of the peroxidase activity of copper ions. Analyst 139:4691–4695
4. Johnson L, Lewis R (2001) Structural basis for control by phosphorylation. Chem Rev 101:2209–2242
5. Liu Y, Xiong E, Li X, Li J, Zhang X, Chen J (2017) Sensitive electrochemical assay of alkaline phosphatase activity based on TdT-mediated hemin/G-quadruplex DNAzyme nanowires for signal amplification. Biosens Bioelectron 87:970–975
6. Zhang Z, Chen Z, Wang S, Cheng F, Chen L (2015) Iodine-mediated etching of gold nanorods for plasmonic ELISA based on colorimetric detection of alkaline phosphatase. ACS Appl Mater Interfaces 7:27639–27645
7. Jiang H, Wang X (2012) Alkaline phosphatase-responsive anodic electrochemiluminescence of CdSe nanoparticles. Anal Chem 84: 6986–6993
8. Liu J, Lin L, Jiao L, Cui M, Wang X, Zhang L, Zheng Z (2012) CdS/$TiO_2$-fluorescein isothiocyanate nanoparticles as fluorescence resonance energy transfer probe for the determination of trace alkaline phosphatase based on affinity adsorption assay. Talanta 98: 137–144
9. Zeng Y, Ren J, Wang S, Mai J, Qu B, Zhang Y, Shen A, Hu J (2017) Rapid and reliable detection of alkaline phosphatase by a hot spots amplification strategy based on well-controlled assembly on single nanoparticle. ACS Appl Mater Interfaces 9:29547–29553
10. Song H, Wang H, Li X, Peng Y, Pan J, Niu X (2018) Sensitive and selective colorimetric detection of alkaline phosphatase activity based on phosphate anion-quenched oxidase-mimicking activity of Ce(IV) ions. Anal Chim Acta 1044:154–161

11. Babson A, Greeley S, Coleman C, Phillips G (1966) Phenolphthalein monophosphate as a substrate for serum alkaline phosphatase. Clin Chem 12:482–490
12. Dehghani Z, Hosseini M, Mohammadnejad J, Bakhshi B, Rezayan A (2018) Colorimetric aptasensor for campylobacter jejuni cells by exploiting the peroxidase like activity of Au@Pd nanoparticles. Microchim Acta 185:448
13. Wu J, Qin K, Yuan D, Tan J, Qin L, Zhang X, Wei H (2018) Rational design of Au@Pt multibranched nanostructures as bifunctional nanozymes. ACS Appl Mater Interfaces 10:12954–12959
14. Wang S, Yan H, Wang Y, Wang N, Lin Y, Li M (2019) Hollow Prussian blue nanocubes as peroxidase mimetic and enzyme carriers for colorimetric determination of ethanol. Microchim Acta 186:738
15. Li W, Fan G, Gao F, Cui Y, Wang W, Luo X (2019) High-activity $Fe_3O_4$ nanozyme as signal amplifier: a simple, low-cost but efficient strategy for ultrasensitive photoelectrochemical immunoassay. Biosens Bioelectron 127:64–71
16. Li S, Zhao X, Yu X, Wan Y, Yin M, Zhang W, Cao B, Wang H (2019) $Fe_3O_4$nanozymes with aptamer-tuned catalysis for selective colorimetric analysis of ATP in blood. Anal Chem 91:14737–14742
17. Yin M, Li S, Wan Y, Feng L, Zhao X, Zhang S, Liu S, Cao P, Wang H (2019) A selective colorimetric strategy for probing dopamine and levodopa through the mussel-inspired enhancement of $Fe_3O_4$ catalysis. Chem Commun 55:12008–12011
18. Ali M, Khalid M, Shah I, Kim S, Kim Y, Lim J, Choi K (2019) Paper-based selective and quantitative detection of uric acid using citrate-capped Pt nanoparticles (PtNPs) as a colorimetric sensing probe through a simple and remote-based device. New J Chem 43:7636–7645
19. Wang H, Li S, Si Y, Zhang N, Sun Z, Wu H, Lin Y (2014) Platinum nanocatalysts loaded on graphene oxide-dispersed carbon nanotubes with greatly enhanced peroxidase-like catalysis and electrocatalysis activities. Nanoscale 6:8107–8116
20. Lin Y, Ren J, Qu X (2014) Catalytically active nanomaterials: a promising candidate for artificial enzymes. Acc Chem Res 47: 1097–1105
21. Wei H, Wang E (2013) Nanomaterials with enzyme-like characteristics (nanozymes): next-generation artificial enzymes. Chem Soc Rev 42:6060–6093
22. Wu T, Hou W, Ma Z, Liu M, Liu X, Zhang Y, Yao S (2019) Colorimetric determination of ascorbic acid and the activity of alkaline phosphatase based on the inhibition of the peroxidase-like activity of citric acid-capped Prussian blue nanocubes. Microchim Acta 186:123
23. Wang C, Gao J, Cao Y, Tan H (2018) Colorimetric logic gate for alkaline phosphatase based on copper (II)-based metal-organic frameworks with peroxidase-like activity. Anal Chim Acta 1004: 74–81
24. Liu B, Huang Z, Liu J (2016) Boosting the oxidase mimicking activity of nanoceria by fluoride capping: rivaling protein enzymes and ultrasensitive $F^-$ detection. Nanoscale 8:13562–13567
25. Jiang L, Fernandez-Garcia S, Tinoco M, Yan Z, Xue Q, Blanco G, Calvino J, Hungria A, Chen X (2017) Improved oxidase mimetic activity by praseodymium incorporation into ceria nanocubes. ACS Appl Mater Interfaces 9:18595–18608
26. Ni P, Chen C, Jiang Y, Zhang C, Wang B, Cao B, Li C, Lu Y (2019) Gold nanoclusters-based dual-channel assay for colorimetric and turn-on fluorescent sensing of alkaline phosphatase. Sensors Actuators B Chem 301:127080
27. Wang X, Zhang Y, Song S, Yang X, Wang Z, Jin R, Zhang H (2016) L-arginine-triggered self-assembly of $CeO_2$ nanosheaths on palladium nanoparticles in water. Angew Chem Int Ed 55:4542–4546
28. Asati A, Santra S, Kaittanis C, Nath S, Perez J (2009) Oxidase-like activity of polymer-coated cerium oxide nanoparticles. Angew Chem Int Ed 48:2308–2312
29. Chen H, Zhou Z, Lu Q, Wu C, Liu M, Zhang Y, Yao S (2019) Molecular structure regulation and enzyme cascade signal amplification strategy for upconversion ratiometric luminescent and colorimetric alkaline phosphatase detection. Anal Chim Acta 1051:160–168
30. Liu H, Li M, Xia Y, Ren X (2017) A turn-on fluorescent sensor for selective and sensitive detection of alkaline phosphatase activity with gold nanoclusters based on inner filter effect. ACS Appl Mater Interfaces 9:120–126
31. Deng J, Yu P, Wang Y, Mao L (2015) Real-time ratiometric fluorescent assay for alkaline phosphatase activity with stimulus responsive infinite coordination polymer nanoparticles. Anal Chem 87:3080–3086
32. Chen C, Yuan Q, Ni P, Jiang Y, Zhao Z, Lu Y (2018) Fluorescence assay for alkaline phosphatase based on ATP hydrolysis-triggered dissociation of cerium coordination polymer nanoparticles. Analyst 143:3821–3828
33. Chen C, Zhang G, Ni P, Jiang Y, Lu Y, Lu Z (2019) Fluorometric and colorimetric dual-readout alkaline phosphatase activityassay based on enzymatically induced formation of colored Au@Ag nanoparticles and an inner filter effect. Microchim Acta 186:10
34. Liu S, Han L, Li N, Xiao N, Ju Y, Li N, Luo H (2018) A fluorescence and colorimetric dual-mode assay of alkaline phosphatase activity via destroying oxidase-like CoOOH nanoflakes. J Mater Chem B 6:2843–2850